H. Teague et al., "Field Results on MIMO Performance in UMB Systems," VTC Spring 2008 - IEEE Vehicular Technology Conference, 2008, pp. 1009-1015, doi: 10.1109/VETECS.2008.216.

Field Results on MIMO Performance in UMB Systems

H. Teague, C. Patel, D. Gore, H. Sampath, A. Naguib, T. Kadous, A. Gorokhov, A. Agrawal

Qualcomm, Inc., San Diego, CA, 92121

Abstract— **The paper presents MIMO field performance results observed using a Ultra Mobile Broadband (UMB) testbed network. We evaluate metrics such as antenna correlations and channel condition number to characterize the MIMO channel. Results show that low condition numbers, which are beneficial to MIMO, are prevalent for a majority of the coverage area in our network. We demonstrate that the use of MIMO provides gains of the order of 20-40% over SIMO transmissions. These gains are made possible by the use of cross-polarized transmit antennas and advanced UMB features that allow dynamic MIMO vs. SIMO transmission selection based on channel conditions. These results are obtained in a truly mobile, wireless wide-area deployment, which makes them unique. Our results point to the viability and value of MIMO in future mobile wireless networks.**

I. Introduction

MIMO techniques are ubiquitous in "next generation" wireless system designs and a significant amount of attention is given to the claimed benefits of this feature in technical as well as marketing literature. The use of MIMO has been spurred by information theoretic results, which promise improved system performance by exploiting wireless channel's spatial dimension [1],[2]. Further, MIMO performance has been extensively studied by both theoretical analysis and lab and field trials [4]-[6]. However, there are few publicly available results that demonstrate the MIMO performance gain achievable in an implementation of a full-featured wide-area wireless broadband access standard operating in a truly mobile environment. This paper attempts to fill this gap with MIMO performance results observed in a UMB testbed network deployed by Qualcomm in San Diego.

UMB (Ultra Mobile Broadband) is an IP-based OFDMA mobile broadband system designed for high speed data and VoIP in a mobile environment that has been standardized in 3GPP2 [7]. UMB achieves very high data rates with high spectral efficiency and incorporates advanced communication techniques like link adaptation and HARQ for high performance with user mobility. In addition, on the forward link (FL), UMB also uses multiple-input multiple-output (MIMO) antennas to achieve higher system capacity and peak data rates. Thus UMB is an ideal system to study MIMO benefits in a wide-area wireless mobile network.

The benefits of MIMO under certain conditions are well known; the more interesting question is how prevalent these conditions are in a real wireless environment. Here, we focus on two primary factors which directly determine the MIMO channel capacity - channel condition number and SNR (defined in section IV). Channel condition number is a measure of the level of spatial diversity and multiplexing capability available in the channel and is a function of deployment characteristics such as transmit (Tx) and receive (Rx) antenna heights, location of scatterers, and Tx and Rx antenna correlations. SNR distribution is also a function of these factors, but additionally depends strongly on the level of interference seen due to loading on the network by other users.

The primary reason for focusing on these two factors separately is that the level of interference in a deployed system can be extremely difficult to predict with confidence. First, the loading seen in a deployed system may change significantly over time, both over the life of the system and over any particular day. Of course loading may also vary significantly from sector to sector in a network. Further, techniques to mitigate interference such as fractional reuse or cancellation may be available depending on competing priorities (for example, complexity, robustness, cost).

Thus, in this paper, we look carefully at channel condition independent of SNR to gauge the "potential" benefits of MIMO. The quantitative achievement of such potential benefits are then dependent on the SNR distribution in the final network, and different proponents/operators may apply their own assumption on interference to reach a final assessment of MIMO benefit.

As an example of potential gains offered by MIMO in a realistic deployment, we show throughput gain results during data collection in our San Diego testbed in lightly loaded conditions.

The remainder of the paper is organized as follows. The trial network is described in Section II. The MIMO implementation is discussed in Section III while the underlying assumptions used for computing MIMO channel metrics are discussed in Section IV. Section V provides detailed field results followed by some conclusions and the scope of future work in Section VI.

II. UMB Trial Network

The trial network consists of five access points (APs), each AP having one 120 degree sector. An FPGA-based prototype access terminal (AT) is mounted in a mobile van. Inter-sector handoffs are supported to provide continuous coverage across different sectors. Some of the key network parameters are

978-1-4244-1645-5/08/$25.00 ©2008 IEEE

listed in Table 1. Our TDD implementation follows the specifications proposed in [8]. However, none of the results here depend on TDD and equivalent results are expected with a FDD UMB system.

To support MIMO, each AP sector utilizes four Tx antennas arranged as two cross-polarized (x-pol) pairs separated by a distance of 3 m (20 wavelengths) The AT van is equipped with two co-polarized, omni-directional roof mounted antennas placed approximately 0.6 m apart as shown in Fig. 1a. These same antennas are also employed in a co-polarized configuration with 0.3 m separation in the interior of our test van. Finally, different form factor accurate (FFA) AT antennas mounted in the interior of our test van were also used for testing purposes. These FFA antennas, illustrated in Fig. 1b, are designed to emulate handset, laptop and computer data card (PC) form factor performance and do not contain any modem hardware.

Table 1. Prototype Parameters

Parameter	Value
Duplexing	TDD, 1:1 FL/RL partitioning
Frequency	2.16-2.18 GHz, 20 MHz bandwidth
AP antennas	4 Tx, 4 Rx
AT antennas	1 Tx, 2 Rx
MIMO	2 layer MIMO supported on FL
FFT Size	2048 (= number of subcarriers)

III. MIMO Implementation

The MIMO transceiver structure used in the prototype is shown in Fig. 2. The prototype implements single codeword (SCW) MIMO transmission [7]. At the transmitter, the encoder and modulator block produces transmit symbols according to the packet format specified by a rate prediction algorithm. The encoded symbols are de-multiplexed to M streams or layers with $1 \le M \le M_T$ where M_T is the number of Tx antennas,

Figure 1. a) AT Antennas mounted on the van roof b) Form factor accurate AT antennas

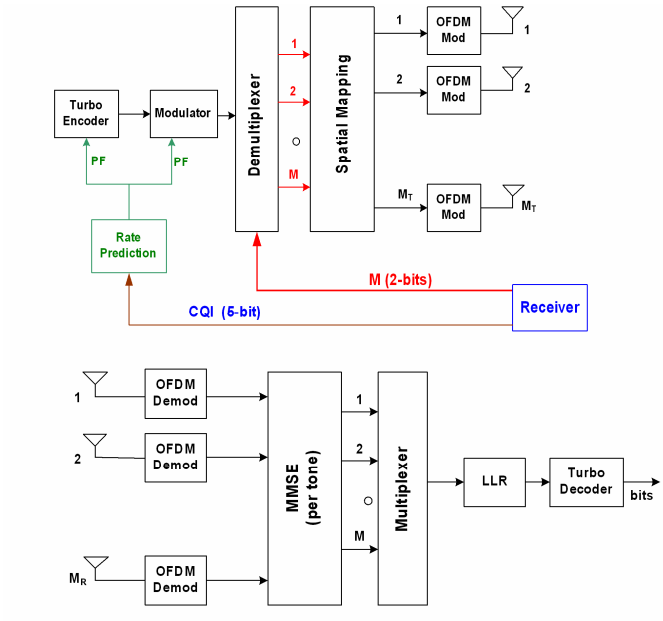

Figure 2. MIMO transceiver

and M is the "rank" of the transmission. Rank one implies a single layer (equivalently SIMO) transmission while a rank greater than one implies multiple layer transmission. After de-multiplexing, the M streams are spatially mapped to M_T Tx antennas by using a set of pseudo-random orthonormal precoding matrices. This precoding is irrelevant to the receiver processing since dedicated pilot symbols per layer are transmitted using the same precoding. The precoding matrices are randomized across frequency and time to increase the level of spatial diversity in the channel. Note that the processing is the same for SIMO transmission, thus single-layer transmissions use all four Tx antennas. Also note that the precoding matrices are formulated to distribute power equally across the Tx antennas. The spatial mapper output is processed using an OFDM modulator. The precoding matrices linearly combine the layer transmission symbols to the physical Tx antennas. Thus, multiple layer symbols are sent simultaneously. However, the degrees of freedom offered by multiple Tx and Rx antennas enables decoding of the different layers at the receiver. A minimum mean square error (MMSE) demodulator is used to demodulate these layers at the receiver.

Depending on the channel conditions such as high spatial correlation, line-of-sight (LOS) conditions and low SNR, MIMO transmission may be inferior to SIMO transmission with a non-capacity-reaching receiver such as MMSE. Therefore, there is also a need to determine whether SIMO or MIMO transmission should be used. This functionality is provided by the rank prediction (or selection) algorithm. The AT estimates the best rank that can be supported for use on the FL by measuring channel quality on the FL CPICH channel, a broadband spatial Common Pilot Channel sent at ~120 Hz. The AT then feeds back the predicted rank along with a channel quality metric to the AP through the Reverse Channel

Quality Information Channel (R-CQICH). This dynamic selection of SIMO or MIMO transmission allows the system to maximize the instantaneous throughput available in a channel with dynamic spatial diversity.

IV. Modeling

Let H be M_R x M_T channel matrix where M_R and M_T are the number of Rx and Tx antennas, respectively. The individual entries h_{ij} of this matrix represent the channel between the Rx antenna *i* and Tx antenna *j*. Note that we estimate broadband, frequency selective channel with a delay resolution of 50 ns chips. Thus, there is a channel matrix corresponding to each channel tap. However, only the four strongest taps estimated at each measurement interval are used to obtain results presented in the next section.

If the channel matrix is orthogonal, then the channel has full rank and can support MIMO. However, channel rank is only a first order and therefore crude measure of the channel capacity [3]. The total capacity depends on the singular values, say λ_i s, of H or equivalently on λ_i^2 s, which are the eigenvalues of HH^*. Among all channels with identical total power (equal Frobenius norm), a channel with identical singular values has the maximum capacity [3]. This degree of closeness of the channel singular values is measured by the channel condition number.

The channel condition number is defined as $\max_i \lambda_i^2 / \min_i \lambda_i^2$. In a sense the channel condition number measures how disparate the performance will be between different eigen- or spatial modes of the channel. Typically, a channel with condition number close to 1 (0 dB using $10\log_{10}(.)$) provides better capacity at high SNR. Such a channel is called a "well-conditioned channel."[1] Therefore, we use channel condition number as a metric to evaluate MIMO channel quality. In addition, Tx and Rx antenna correlation metrics are also used.

A. Metric computation

Field data was collected by driving the mobile AT van along a pre-defined drive route near the Qualcomm campus in San Diego. To evaluate the condition number and correlation metrics, the channel matrix was computed using CPICH channel estimates collected on the drive route. For computing correlation coefficients, the drive route was divided into geographical bins of approximately 5 m. A smaller geographical bin would give better spatial resolution. However, to obtain adequate number of samples to average over fading statistics and filter out noise effects, we chose a bin size of 5 m. It is reasonable to assume that the scattering environment does not change significantly across the 5 m bins. (Note that a bin size of 3 to 7 m was used in [5]). A receive correlation matrix $R_{rx} = (1/M_T)E[HH^*]$ was computed at each bin by averaging HH^* obtained from multiple snapshots of the max-tap H within this bin (E and * are the expectation and complex conjugate transpose operators, respectively).

Correlation coefficient, ρ, was computed from the covariance matrix $\hat{R}$.

$$\hat{R} = R_{rx} - (1/M_T)\left[E(H)E(H)^*\right]$$

$$\rho_{rx} = \hat{R}_{12} / \sqrt{\hat{R}_{11}\hat{R}_{22}}$$

The Tx correlation coefficient was computed in a similar fashion by computing the covariance matrix using the transmit correlation matrix $R_{tx} = (1/M_R)E[H^*H]$.

The condition numbers were computed by eigenvalue decomposition of HH^* for each sample of H estimated along the drive route. Unlike the correlation computation, no averaging of HH^* was done over geographical bins. The instantaneous channel capacity depends on the channel eigenvalues and therefore the condition number of the instantaneous channel H. Also, high CPICH processing gain provides high SNRs for channel estimates. Therefore, no averaging over bins is done for computing the condition numbers.

V. Field Results

A. Spatial channel measurements

1) Transmit antenna correlation

Consider the 4 Tx antenna configuration shown in Fig. 3.

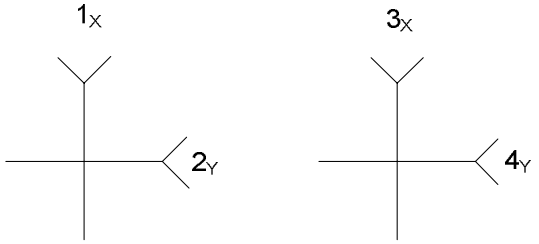

Figure 3. Transmit antenna configuration

The x-pol antenna pairs (1,2) and (3,4) are on spatially separated panels. The pair (1,3) is co-polarized, but x-polarized with respect to the pair (2,4). Now, we compute the cumulative distribution function (cdf) of AP Tx antenna correlation coefficient obtained with measurements from the roof-mounted and the handset Rx (Fig. 4 and 5). The AP Tx correlation is

[1] Fften in the existing literature, the condition number is defined as $\max_i \lambda_i / \min_i \lambda_i$ i.e., as the ratio of the singular values of H rather than $\max_i \lambda_i^2 / \min_i \lambda_i^2$.

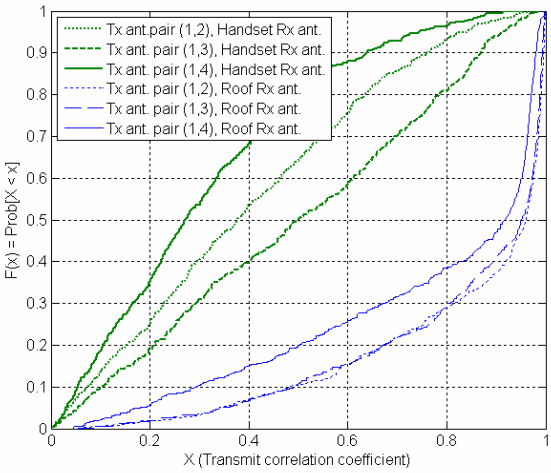

Figure 4. AP Tx antenna correlation coefficient cdf computed using the strongest channel tap

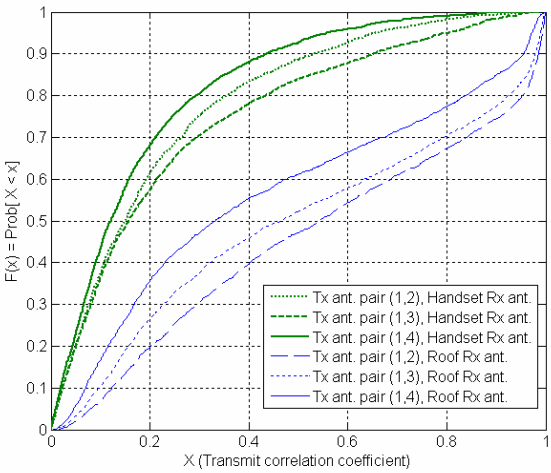

Figure 5. AP Tx antenna correlation coefficient cdf computed using four strongest channel taps

computed using three different Tx antenna pairs to compare and contrast the correlation using these pairs. The cdf is computed using the strongest channel tap and four strongest channel taps[2] measured at each sampling instant across the drive route.

The four strongest channel tap cdf is obtained by calculating four correlation coefficients, one each for a distinct channel tap and using all the four coefficients to obtain the overall cdf. It is evident that the x-pol antenna pair, especially the spatially separated one, has lower correlation than the co-pol pair. Further, the transmit correlation is different when measured with receive handset and roof antennas. This suggests that the separability of transmit and receive correlation often assumed in the literature is not applicable to these measurements.

2) Receive antenna correlation

Fig. 6 and 7 plot the cdfs of the Rx correlation coefficient computed using the strongest channel tap and four strongest channel taps, respectively. Note that the four taps cdfs show lower correlation compared to the single tap cdfs. This difference is more pronounced for the roof-top antennas. This is likely due to the presence of LOS component in the strongest tap.

While it is reasonable to expect higher correlation in the more closely spaced FFA antennas, it is interesting to note that this is clearly not the case in this data. Possible reasons for the lower correlation observed could be the placement of the FFA

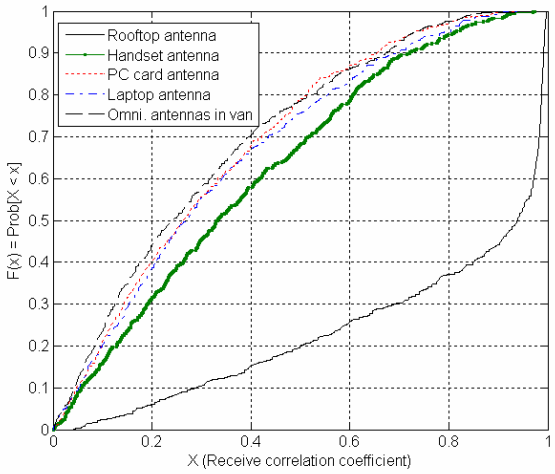

Figure 6. Receive antenna correlation cdf computed using the strongest channel tap

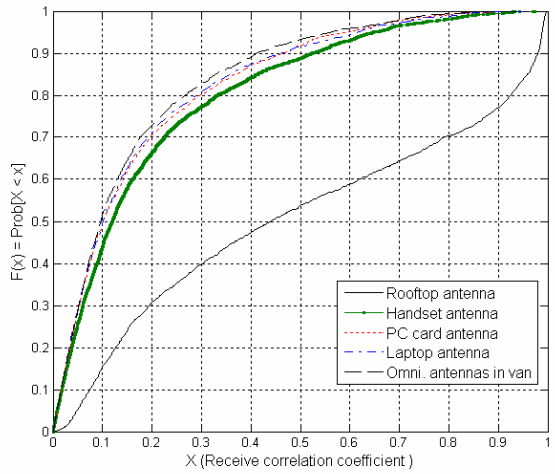

Figure 7. Receive antenna correlation cdf computed using four strongest channel taps

antennas in the interior of the van, and the potential for

[2] Four channel taps are used in addition to single max tap because the max tap is often dominated by line-of-sight channel with high correlation. Thus, the single tap results can be pessimistic for evaluating MIMO potential.

additional polarization diversity relative to the aligned monopoles of the roof-top antennas. However, the exact cause has not been fully isolated. The correlations of FFA antennas are similar to omni antennas inside the van. The roof antennas, though spatially separated, have higher elevation and are likely to see more LOS conditions with less local scattering. Therefore, they have relatively higher correlation. Nevertheless, these results indicate that appropriately designed FFA antennas can be quite suitable for MIMO transmissions.

3) Condition number

The condition numbers observed with receive roof antennas for the strongest channel tap and the four strongest channel taps[3] are provided in Fig. 8 and 9, respectively. Comparing results in Fig. 8 and 9, it is evident that the condition numbers are better with more channel taps. The strongest channel tap is more likely to have higher LOS contribution compared to other taps. This leads to higher condition numbers for the strongest channel tap. These results suggest that weaker taps can contribute to MIMO capacity gains by providing better channel condition. Fig. 8 and 9 also plot the condition numbers computed using various 2 Tx antennas pairs. These are computed by picking the two columns corresponding the two antennas from the 2x4 channel matrix H and performing an eigenvalue decomposition of this reduced 2x2 matrix. We notice that the co-pol antenna pair (1,3) (curve C) has higher condition number than the x-pol pairs (1,2) and (1,4) (curves B and D). Though the co-pol pair is 20 wavelengths apart, the lack of local scattering around the elevated AP Tx antennas

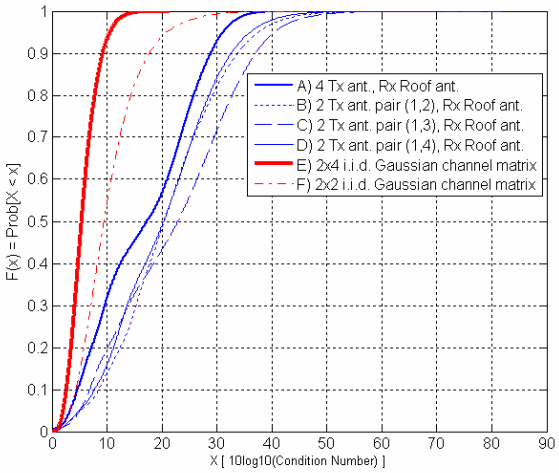

Figure 8. Condition numbers computed using the strongest channel tap and Rx roof antennas

[3] The conditions numbers are computed separately for each channel tap and used to compute the overall cdf.

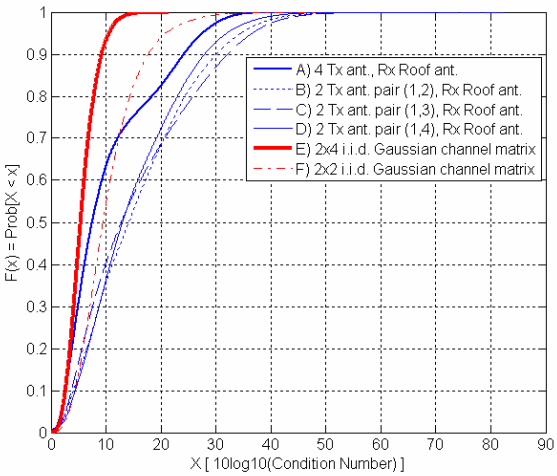

Figure 9. Condition numbers computed using four strongest channel taps and Rx roof antennas

likely results in higher condition number for this pair. The improvement in condition number by using x-pols compared to co-pols is more evident in Fig. 10, where we plot condition number results obtained using handset FFA antennas on the receive side. This demonstrates the value of using x-pol Tx antennas for MIMO. Further, the condition numbers with 4 Tx antennas (curve A) are universally better than those with 2 Tx antenna (curves B, C, and D), showing that additional Tx antennas (even co-polarized) can provide substantial improvements.

For reference, distributions of condition numbers for matrices with independent and identically distributed (i.i.d) Gaussian elements are also provided as a lower bound since such matrices represent the ideal channel for MIMO capacity. The 2x4 and 2x2 cases are shown (curves E and F).

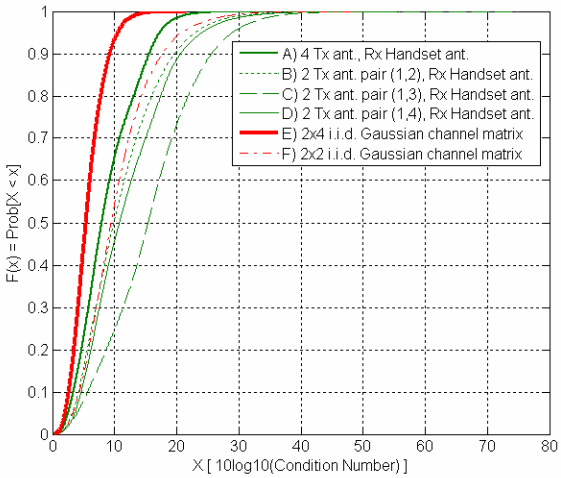

Figure 10. Condition numbers computed using the strongest channel tap and Rx handset antennas

DOCKET ALARM

Explore Litigation Insights

Docket Alarm provides insights to develop a more informed litigation strategy and the peace of mind of knowing you're on top of things.

Real-Time Litigation Alerts

Keep your litigation team up-to-date with **real-time alerts** and advanced team management tools built for the enterprise, all while greatly reducing PACER spend.

Our comprehensive service means we can handle Federal, State, and Administrative courts across the country.

Advanced Docket Research

With over 230 million records, Docket Alarm's cloud-native docket research platform finds what other services can't. Coverage includes Federal, State, plus PTAB, TTAB, ITC and NLRB decisions, all in one place.

Identify arguments that have been successful in the past with full text, pinpoint searching. Link to case law cited within any court document via Fastcase.

Analytics At Your Fingertips

Learn what happened the last time a particular judge, opposing counsel or company faced cases similar to yours.

Advanced out-of-the-box PTAB and TTAB analytics are always at your fingertips.

API

Docket Alarm offers a powerful API (application programming interface) to developers that want to integrate case filings into their apps.

LAW FIRMS
Build custom dashboards for your attorneys and clients with live data direct from the court.

Automate many repetitive legal tasks like conflict checks, document management, and marketing.

FINANCIAL INSTITUTIONS
Litigation and bankruptcy checks for companies and debtors.

E-DISCOVERY AND LEGAL VENDORS
Sync your system to PACER to automate legal marketing.